Proceedings of CONF-MCEE 2026 Symposium: Advances in Sustainable Aviation and Aerospace Vehicle Automation
DOI: 10.54254/2755-2721/2026.KA26967

Effects of CO_2 on Elastic Characteristics of Fluid-Saturated Sandstone

Yuxi Duan

Department of Geology, Northwestern University, Xi'an, China
13186139186@163.com

Abstract. Currently, investigating the mechanism by which CO_2 affects the elastic response of porous media is of significant scientific value for ensuring the safety and efficiency of CCUS injection operations. However, existing studies have inadequately considered the mixing effects of CO_2 and other fluids, and there is a paucity of quantitative research on the elastic parameters of sandstone under varying CO_2 properties. To address this, we employ a rock physics modeling approach. Firstly, we estimate the equivalent elastic parameters of the rock matrix using the VRH averaging method. Subsequently, we utilize the Krief model to quantify the influence of pores on the elastic characteristics of the rock skeleton, and simulate the elastic properties of the CO_2-water mixed fluid via the Brie model. Finally, we couple the influence of the mixed fluid with Biot-Gassmann theory to construct a rock physics model for saturated sandstones, and further calculate their elastic moduli as well as P-wave and S-wave velocities. We investigate the laws governing how porosity, CO_2 saturation, and density affect the elastic parameters of sandstone. The results indicate that with increasing porosity, the rock's bulk modulus, shear modulus, and P-wave and S-wave velocities decrease; following CO_2 injection, both CO_2 saturation and density exert an influence on the rock's elastic parameters: the higher the CO_2 saturation, the smaller the rock's bulk modulus, while the P-wave velocity first decreases and then increases, the S-wave velocity increases, and the shear modulus is independent of CO_2 properties; the greater the CO_2 density, the smaller the bulk modulus and P-wave and S-wave velocities, with the shear modulus remaining essentially unchanged.

Keywords: CO_2, elastic characteristics, porosity, saturation, density

1. Introduction

Carbon Capture, Utilization, and Storage (CCUS) holds a critical strategic position in carbon emission control and the realization of carbon neutrality goals [1-3]. As a key component of the CCUS technology system, investigating the multi-physical field response characteristics of formations induced by CO_2 injection processes is of substantial scientific value and practical guiding significance for ensuring the safety and efficiency of injection operations. Its research progress directly impacts the advancement of carbon emission governance and the achievement of carbon neutrality goals [4-6].

© 2026 The Authors. This is an open access article distributed under the terms of the Creative Commons Attribution License 4.0 (https://creativecommons.org/licenses/by/4.0/).

DOI: 10.54254/2755-2721/2026.KA26967

Research on CO_2 storage has been extensively conducted across various fields, primarily focusing on the mechanisms by which CO_2 injection affects rock properties, the optimization of migration and storage conditions, and the development of related application technologies [7-10]. Zhao et al. [11] performed laboratory experiments on CO_2 displacement of natural cores under simulated reservoir conditions and observed that, following CO_2 injection, acidic fluids formed by dissolution in water react with minerals, leading to significant changes in rock pore structure (with increased proportions of both small and large pores), permeability (gradual increase), and wettability (enhanced hydrophilicity). Xu et al. [12] confirmed through experiments that the migration rate and saturation of CO_2 in rocks are regulated by factors such as effective stress, reservoir pressure, and temperature, exhibiting significant variations in heterogeneous rocks. Ye [13] noted that the CCUS compressor developed by Jichai Power has been promoted and applied in numerous domestic CCUS-EOR (Enhanced Oil Recovery) demonstration projects and pilot tests. Regarding the influence of CO_2 injection on rock elastic characteristics, Ali et al. [14] conducted experiments on Berea sandstone with a quartz content of approximately 90% and found that CO_2 injection can reduce rock strength by 10–15%, increase permeability by up to 100%, enhance porosity by 10%, and elevate the elastic creep rate by more than twofold. Additionally, the poroelastic modulus measured via triaxial compression experiments and the elastic characteristics related to the load-induced fracture process analyzed using acoustic emission data in uniaxial compression experiments are significantly affected. However, existing studies have inadequately considered the mixing effects of CO_2 and other fluids, and there is a scarcity of research on the elastic response characteristics of sandstone reservoirs during geological storage.

Therefore, this study employs a rock physics modeling approach to explore the mechanism underlying the influence of CO_2 on rock elastic responses. Firstly, the VRH (Voigt-Reuss-Hill) averaging method is utilized to estimate the equivalent elastic parameters of the rock matrix (including mineral phases). Secondly, the Krief model is applied to quantify the impact of pores on the elastic characteristics of the rock skeleton. On this basis, the Biot-Gassmann theory is used to implement the replacement calculation of CO_2-water mixed fluids, thereby constructing a rock physics model for saturated sandstone reservoirs. Through the aforementioned research, the influence laws of CO_2 saturation and density on rock elastic modulus and velocity are investigated, aiming to provide a theoretical basis for CO_2 geological storage in sandstone reservoirs.

2. Rock physics model for CO_2 injection

This paper proposes a rock physics model for CO_2 injection in sandstones to simulate the quantitative influence of parameters such as CO_2 saturation and density on rock elastic modulus and velocity, including four steps (the specific process is shown in Figure 1):

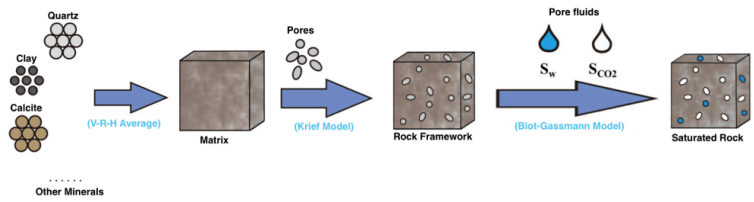

Figure 1. Rock physics modeling process for CO_2 injection

1) Considering the rock matrix from minerals, the VRH (Voigt - Reuss - Hill) averaging method is used to estimate the equivalent elastic parameters (including Young's modulus, shear modulus,

DOI: 10.54254/2755-2721/2026.KA26967

etc.) of the rock matrix (including mineral phases); this process assumes that each component of the rock is isotropic and linearly elastic.

The Voigt boundary is the weighted sum of the elastic moduli of each phase according to the volume fraction under the condition of equal strain, which is the theoretical upper limit (1):

$$E_{voigt} = \sum_{i=1}^{n} f_i E_i \tag{1}$$

Where, fi is the volume fraction of the i - th phase, and Ei is the elastic modulus of the i - th phase.

The Reuss boundary is the harmonic average of the elastic moduli of each phase weighted by the volume fraction under the condition of equal stress, which is the theoretical lower limit (1):

$$\frac{1}{E_{Reuss}} = \sum_{i=1}^{n} \frac{f_i}{E_i} \tag{2}$$

Where, fi is the volume fraction of the i - th phase, and Ei is the elastic modulus of the i - th phase.

The VRH average is the arithmetic mean of the above upper and lower bounds (3):

$$E_{VRH} = \frac{E_{voigt} + E_{Reuss}}{2} \tag{3}$$

2) Considering the rock skeleton from pores, the Krief model is used to quantify the influence of pores on the elastic characteristics of the sandstone skeleton; the Krief model constructs the following formulas through rock physics measured data and theoretical derivation [15, 16]:

$$K_{dry} = K_0(1-\varphi)^{3/(1-\varphi)} \tag{4}$$

$$G_{dry} = G_0(1-\varphi)^{3/(1-\varphi)} \tag{5}$$

Where K_{dry} and G_{dry} are the bulk modulus and shear modulus of the sandstone skeleton, respectively, K_0 and G_0 are the bulk modulus and shear modulus of the rock matrix, respectively, and φ is the rock porosity.

3) The Brie model is used to mix CO_2, water, and oil three - phase fluids; for the gas - water two - phase saturation case (6):

$$K_{fl} = (K_w - K_g) \cdot S_w^e + K_g \tag{6}$$

Where, K_w is the bulk modulus of water, K_g is the bulk modulus of gas, S_w is the water saturation in the gas - water mixture, e is the Brie coefficient, which is set to 1 in this study.

4) The Biot - Gassmann model is used for fluid substitution to fill water and CO_2 fluids into the dry rock skeleton, and then the bulk modulus and shear modulus can be obtained, which are finally combined with density to convert into P - wave and S - wave velocities. The Biot theory considers the influence of fluid inertia and viscosity on the basis of the Gassmann theory. It mainly describes the relationship between the bulk modulus of fluid - saturated rocks and the skeleton modulus, pore fluid modulus, and porosity, that is:

$$\frac{K_{sat} - K_{dry}}{K_{fl} - K_{dry}} = \frac{\Phi(K_0 - K_{dry})}{K_0(1-\Phi)K_{dry} + \Phi K_0 K_{fl}} \tag{7}$$

DOI: 10.54254/2755-2721/2026.KA26967

Where, K_{sat} is the bulk modulus of the saturated rock, K_{dry} is the bulk modulus of the dry rock, K_{fl} is the bulk modulus of the pore fluid, K_0 is the bulk modulus of the rock skeleton mineral, and is the Φ porosit.

3. Simulation results

3.1. Influence of porosity on elastic parameters

To analyze the influence of porosity on the elastic modulus of rocks, the porosity was varied from 0% to 100% and CO_2 saturation from 0% to 30%. Figures 2(a) and 2(b) illustrate the variation patterns of the rock's bulk modulus and shear modulus under different porosities and CO_2 saturations. As shown in the figures, under a constant CO_2 saturation, both the bulk modulus and shear modulus decrease to varying degrees with increasing porosity, exhibiting a trend of a rapid initial decline followed by a slower decrease. At a fixed porosity, variations in CO_2 saturation reveal that a higher CO_2 saturation corresponds to a lower bulk modulus, and vice versa, with this trend being particularly evident when the CO_2 saturation is 0%. For the shear modulus, it remains consistent across different CO_2 saturations at the same porosity. In summary, a higher rock porosity (i.e., a looser rock structure) results in smaller bulk and shear moduli (indicating greater compressibility), while a higher CO_2 content leads to a smaller bulk modulus (greater compressibility) with the shear modulus remaining unchanged.

Regarding the variations of P-wave and S-wave velocities with porosity under different CO_2 saturation conditions, the porosity was set in the range of 0% to 100% and CO_2 saturation in 0% to 30%. Figures 2(c) and 2(d) depict the variation patterns of P-wave and S-wave velocities under these conditions. It can be observed from the figures that under a constant CO_2 saturation, both P-wave and S-wave velocities decrease to varying degrees with increasing porosity, showing a trend of a rapid initial decline followed by a slower decrease. At a fixed porosity, with changes in CO_2 saturation, the P-wave velocity reaches its maximum when the CO_2 saturation is 0%, while other P-wave velocities and all S-wave velocities increase with increasing CO_2 saturation.

This phenomenon can be explained as follows: P-wave propagation depends on the bulk modulus of the medium, with a larger bulk modulus corresponding to a higher P-wave velocity. When the CO_2 saturation is 0%, pores are typically saturated with water (or other fluids such as crude oil), and the bulk modulus of water is significantly higher than that of CO_2 (including gaseous and supercritical CO_2). For other saturation levels, the increase in both P-wave and S-wave velocities with rising CO_2 saturation is attributed to the lower density of CO_2 compared to water. As CO_2 displaces other pore fluids, the average density of the mixed pore fluid decreases. Since S-wave propagation primarily relies on the shear modulus and is highly sensitive to fluid density, a reduction in fluid density weakens the shear effect on the rock skeleton, resulting in less energy loss and thus a higher S-wave velocity. For P-wave velocity, although CO_2 has a lower density than water, CO_2 may exist in a high-pressure (supercritical) state, where its bulk modulus increases with pressure. Meanwhile, the influence of the reduced density of the mixed fluid may outweigh that of the decreased bulk modulus, leading to an increase in P-wave velocity with rising CO_2 saturation.

DOI: 10.54254/2755-2721/2026.KA26967

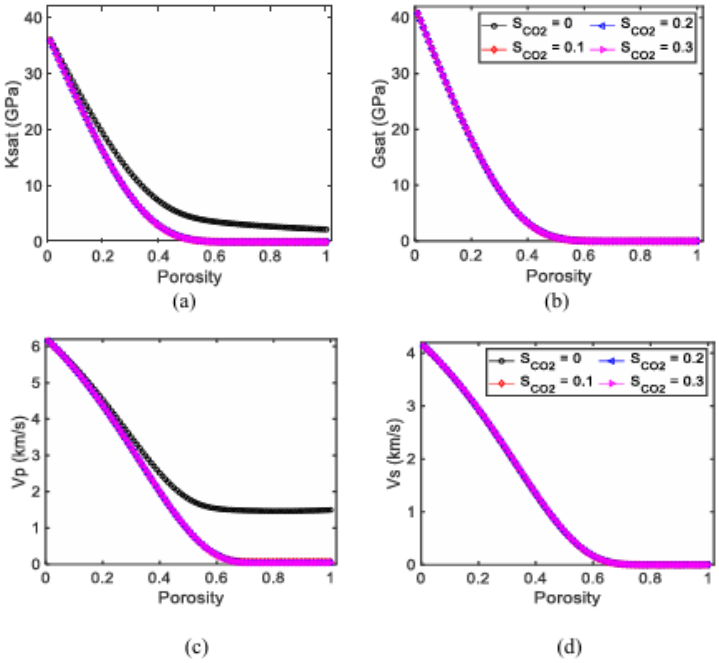

Figure 2. Variation of bulk modulus, shear modulus, P - wave and S - wave velocities with porosity under different CO_2 saturations (a) Bulk modulus; (b) Shear modulus (c) P - wave velocity; (d) S - wave velocity

3.2. Influence of CO_2 saturation on elastic parameters

To analyze the influence of CO_2 saturation on the elastic modulus and velocity of rocks, the porosity was set in the range of 5% to 20% and CO_2 saturation in 0% to 100%. Figure 3 illustrates the variation patterns of bulk modulus, shear modulus, as well as P-wave and S-wave velocities with CO_2 saturation under different porosities. As shown in Figures 3(a) and 3(b), at a constant porosity, with increasing CO_2 saturation, the bulk modulus first undergoes a linear rapid decline (when CO_2 saturation is 0%–1%) followed by a linear slow decline. In contrast, the shear modulus remains essentially stable as CO_2 saturation increases. For a given CO_2 saturation, both the bulk modulus and shear modulus exhibit a decreasing trend with increasing porosity. In summary, a higher CO_2 saturation in the rock corresponds to a smaller bulk modulus, while the shear modulus remains largely unchanged; a larger porosity leads to smaller bulk and shear moduli.

Regarding the variations of P-wave and S-wave velocities with CO_2 saturation under different porosities (with porosity ranging from 5% to 20% and CO_2 saturation from 0% to 100%), Figures 3(c) and 3(d) depict the respective variation patterns. It can be observed from these figures that at a constant porosity, with increasing CO_2 saturation, the P-wave velocity first shows a linear rapid decline (when CO_2 saturation is 0%–1%) and then a linear slow increase. The S-wave velocity, on the other hand, exhibits a linear slow increase, with a steeper rising slope for larger porosities. For a given CO_2 saturation, both P-wave and S-wave velocities decrease as porosity increases.

DOI: 10.54254/2755-2721/2026.KA26967

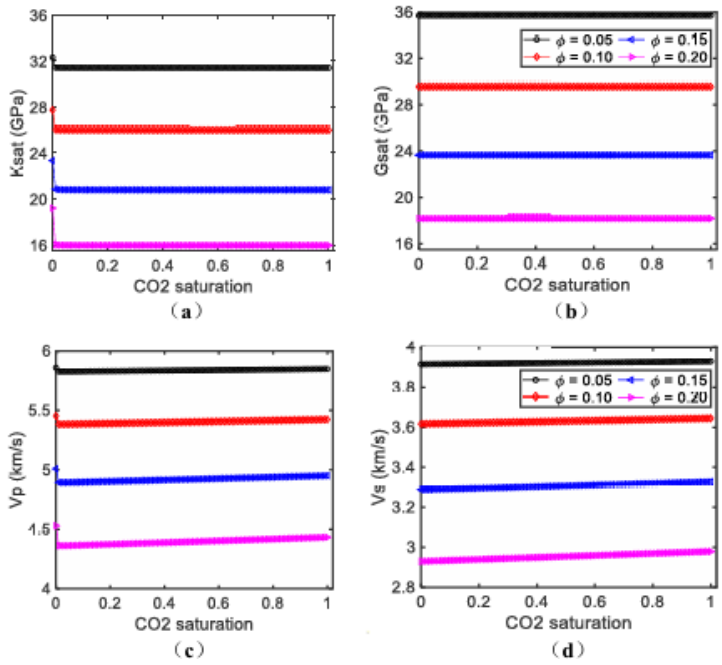

Figure 3. Variation of bulk modulus, shear modulus, P - wave and S - wave velocities with CO_2 saturation under different porosities (a) Bulk modulus; (b) Shear modulus (c) P - wave velocity; (d) S - wave velocity

3.3. Influence of CO_2 density on elastic parameters

To analyze the influence of CO_2 density on the elastic modulus and velocity of rocks, the porosity was set in the range of 5% to 20% and CO_2 density in 0 to 1200 kg/m³. Figure 4 illustrates the variation patterns of bulk modulus, shear modulus, as well as P-wave and S-wave velocities with CO_2 density under different porosities. As shown in Figures 4(a) and 4(b), at a constant porosity, the bulk modulus exhibits a slow decreasing trend with increasing CO_2 density. In contrast, the shear modulus remains essentially stable as CO_2 density increases. For a given CO_2 density, both the bulk modulus and shear modulus show a decreasing trend with increasing porosity. In summary, a higher CO_2 density in the rock corresponds to a smaller bulk modulus, while the shear modulus remains largely unchanged; a larger porosity leads to smaller bulk and shear moduli.

Regarding the variations of P-wave and S-wave velocities with CO_2 density under different porosities (with porosity ranging from 5% to 20% and CO_2 density from 0 to 1200 kg/m³), Figures 4(c) and 4(d) depict the respective variation patterns. It can be observed from these figures that at a constant porosity, both P-wave and S-wave velocities undergo a linear slow decline with increasing CO_2 density, and the larger the porosity, the higher the decline rate. For a given CO_2 density, both P-wave and S-wave velocities decrease as porosity increases.

DOI: 10.54254/2755-2721/2026.KA26967

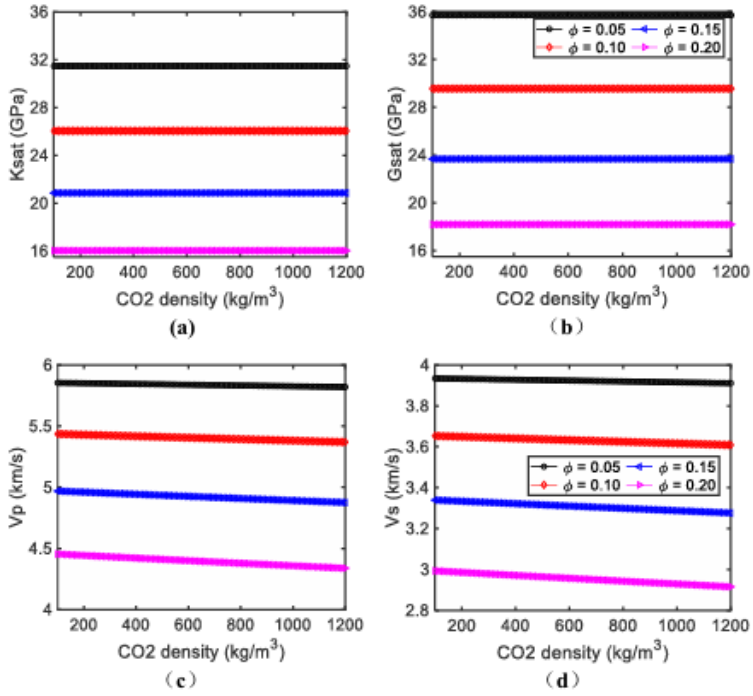

Figure 4. Variation of bulk modulus, shear modulus, P - wave and S - wave velocities with CO_2 density under different porosities (a) Bulk modulus; (b) Shear modulus (c) P - wave velocity; (d) S - wave velocity

4. Conclusions

4.1. Influence of porosity on elastic parameters

Under a constant CO_2 saturation, with increasing porosity, the bulk modulus, shear modulus, P-wave velocity, and S-wave velocity all exhibit a trend of a rapid initial decline followed by a slow decrease. At a fixed porosity, a higher CO_2 saturation corresponds to a smaller bulk modulus; in contrast, the shear modulus remains unaffected by CO_2 saturation for the same porosity. For the P-wave velocity, it reaches its maximum when the CO_2 saturation is 0% and increases with rising CO_2 saturation under other conditions. The S-wave velocity increases as CO_2 saturation rises.

4.2. Influence of CO_2 saturation on elastic parameters

At a constant porosity, with increasing CO_2 saturation, the bulk modulus first undergoes a rapid linear decrease (within the saturation range of 0%–1%) and then a slow linear decrease. The shear modulus remains essentially stable. The P-wave velocity initially shows a rapid linear decrease (within 0%–1% saturation) followed by a slow linear increase. The S-wave velocity increases slowly in a linear manner, with a steeper rising slope for larger porosities. For a given CO_2 saturation, a larger porosity results in smaller bulk modulus, shear modulus, P-wave velocity, and S-wave velocity.

4.3. Influence of CO_2 density on elastic parameters

Under a constant porosity, with increasing CO_2 density, the bulk modulus decreases slowly, while the shear modulus remains basically unchanged. Both the P-wave and S-wave velocities exhibit a

DOI: 10.54254/2755-2721/2026.KA26967

relatively slow linear decrease, with a higher rate of decrease for larger porosities. For a given CO_2 density, a larger porosity leads to smaller bulk modulus, shear modulus, P-wave velocity, and S-wave velocity.

References

[1] Vialle S, Vanorio T. Laboratory measurements of elastic properties of carbonate rocks during injection of reactive CO2-saturated water [J]. Geophysical Research Letters, 2011, 38(1).

[2] Turkson J N, Md Yusof M A, Fjelde I, et al. Carbonated water injection for enhanced oil recovery and CO2 geosequestration in different CO2 repositories: a review of physicochemical processes and recent advances [J]. Energy & Fuels, 2024, 38(8): 6579-6612.

[3] Wang J, Wang H, Wang X, et al. A multiphysical-geochemical coupling model for caprock sealing efficiency in CO2 geosequestration [J]. Deep Underground Science and Engineering, 2023, 2(2): 188-203.

[4] Bello A, Ivanova A, Cheremisin A. A comprehensive review of the role of CO2 foam EOR in the reduction of carbon footprint in the petroleum industry [J]. Energies, 2023, 16(3): 1167.

[5] Wang W, Liang Z, Zuo J, et al. The pore structure changes and CO2 migration dynamic characteristics in tight sandstone during supercritical CO2 geosequestration: A case study in the Chang 7 layer, Ordos Basin, China [J]. Fuel, 2025, 379: 133019.

[6] Aminaho E N, Hossain M, Faisal N H, et al. Application of machine learning in the determination of rock brittleness for CO2 geosequestration [J]. Machine Learning with Applications, 2025: 100656.

[7] Sharifi J. Geophysical monitoring of CO2 storage using rock physics template [J]. Geoenergy Science and Engineering, 2025, 250: 213808.

[8] Fawad M, Mondol N H. Monitoring geological storage of CO2 using a new rock physics model [J]. Scientific Reports, 2022, 12(1): 297.

[9] Dong Y J, Shen Y, Guo K, et al. Characterization of petrophysical and seismic properties for CO2 storage with sensitivity analysis [J]. Petroleum Science, 2025, 22(1): 193-209.

[10] Mawa Tuzingila R, Kong L, Koy Kasongo R. Investigation of the Mineral Content and Geomechanical Behaviors of Shale Gas Reservoirs after CO2 Injection Using Rock Physics Modeling [J]. International Journal of Geomechanics, 2025, 25(10): 04025217.

[11] Zhao G M, Yang Y Z, Yang H Y. Changes of Rock Properties in CO_2 Flooding [J]. Science & Technology Review, 2013, 23: 50-52.

[12] Xu L，Li Q，Myers M，Tan Y S，He M，Li X C. The effects of porosity and permeability changes on simulated supercritical CO2 migration front in tight glutenite under different effective confining pressures from 1.5 MPa to 21.5 MPa. Greenhouse Gases [J]. Science and Technology, 2021, 11: 19-36.

[13] Ye, Y. P. Supercritical CO_2 Injection Compressor Supports the Development of the CCUS Industry [J]. Petroleum Knowledge, 2025, 3: 32-33.

[14] Tarokh A, Makhnenko R Y, Kim K, et al. Influence of CO_2 injection on the poromechanical response of Berea sandstone [J]. International Journal of Greenhouse Gas Control, 2020, 140: 10.1016.

[15] Krief M, Garat J, Stellingwerff J, Ventre J. A petrophysical interpretation using the velocities of P and S waves (full-waveform sonic) [J]. The Log Analyst, 1990, 31: 355-369.

[16] Mavko G, Mukerji T. Comparison of the Krief and critical porosity models for prediction of porosity and Vp/Vs [J]. Geophysics, 1998, 63: 925-927.